Chemosphere 304 (2022) 135347

Contents lists available at ScienceDirect

Chemosphere

journal homepage: www.elsevier.com/locate/chemosphere

2011–2020 trends of urban and regional ammonia in and around Barcelona, NE Spain

C. Reche [a,*], N. Pérez [a], A. Alastuey [a], N. Cots [b], E. Pérez [b], X. Querol [a]

[a] IDAEA-CSIC, Barcelona, Spain
[b] Departament de Territori i Sostenibilitat, Generalitat de Catalunya, Barcelona, Spain

HIGHLIGHTS

- Availability of NH_3 measurements in urban environments is scarce in Europe.
- A ten-year dataset on multi-site NH_3 concentrations in NE Spain was evaluated.
- NH_3 concentrations ranged between 0.9 and 5.3 μgm^{-3}, with the highest at the traffic site.
- Concentrations increased over time at the urban and the mountain sites, especially during summers.
- Increases in NH_3 may be responsible for the lack of a decreasing trend of NO_3^-, despite NO_2 reductions.

GRAPHICAL ABSTRACT

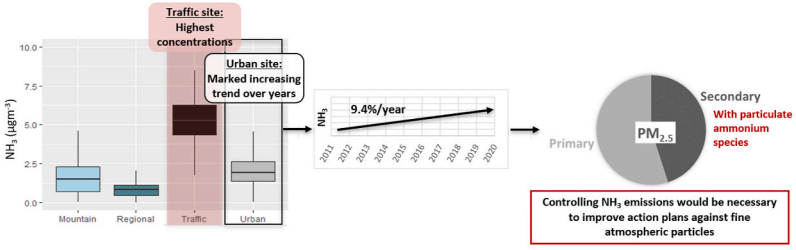

ARTICLE INFO

Handling Editor: Volker Matthias

Keywords:
NH_3
Secondary inorganic particles
Time trends
Air pollution abatement measures
Fine atmospheric particles

ABSTRACT

It is well established that in environments where NH_3 abundance is limiting in secondary $PM_{2.5}$ generation, a reduction of NH_3 emissions can result in an important contribution to air quality control. However, as deduced from open data published by the European Environmental Agency, the availability of measurements of NH_3 concentrations is very scarce, with very few countries in Europe reporting data consistently for extensive periods, this being especially true for urban background sites. In this framework, simultaneous multi-site measurements were carried out in NE (Northeast) Spain from 2011 to 2020, using diffusion tubes. The highest NH_3 concentrations were recorded at the traffic site (5.3 μgm^{-3} on average), followed by those measured at the urban background site (2.1 μgm^{-3}). Mean concentrations at the mountain site were 1.6 μgm^{-3}, while the lowest concentrations were recorded at the regional site (0.9 μgm^{-3}). This comparison highlights traffic emissions as an important source of NH_3. A statistically significant time trend of this pollutant was observed at the urban background site, increasing by 9.4% per year. A season-separated analysis also revealed a significant increasing trend at the mountain site during summer periods, probably related with increasing emissions from agricultural/livestock activities. These increases in NH_3 concentrations were hypothesized to be responsible for the lack of a decreasing trend of NO_3^- concentrations at the monitoring sites, in spite of a markedly reduction of NO_2 during the period, especially at the urban background. Thus, this would in turn affect the effectiveness of current action plans to abate fine aerosols, largely made up of secondary compounds. Actions to reduce NH_3 concentrations at urban backgrounds are challenging though, as predicting NH_3 is subjected to a high uncertainty and complexity due to its dependence on a variety of factors. This complexity was clearly indicated by the application of a decision tree algorithm to find the parameters better predicting NH_3 at the urban background under study. O_3,

* Corresponding author.
E-mail address: cristina.reche@idaea.csic.es (C. Reche).

https://doi.org/10.1016/j.chemosphere.2022.135347
Received 11 February 2022; Received in revised form 8 June 2022; Accepted 12 June 2022
Available online 14 June 2022
0045-6535/© 2022 The Authors. Published by Elsevier Ltd. This is an open access article under the CC BY-NC-ND license (http://creativecommons.org/licenses/by-nc-nd/4.0/).

NO, NO_2, CO, SO_2 and OM + EC concentrations, together with meteorological indicators, were used as independent variables, obtaining no combination of parameters evidently able to predict significant differences in NH_3 concentrations, with a coefficient of determination between real and predicted measurements lower than 0.50. This emphasizes the need for highly temporally and spatially resolved NH_3 measurements for an accurate design of abatement actions.

1. Introduction

NH_3 is the only primary basic gas species in the atmosphere, being crucial in atmospheric chemical and geochemical processes. Ammonia reacts quickly with sulfuric (H_2SO_4) and nitric (HNO_3) acids to contribute to ambient levels of fine particles. Ammonia preferentially neutralize H_2SO_4 to form ammonium sulfate ($(NH_4)_2SO_4$) and ammonium bisulphate (NH_4HSO_4). Excess NH_3 is then available to form ammonium nitrate (NH_4NO_3) from HNO_3 or ammonium chloride (NH_4Cl) from hydrochloric acid (HCl).

Ammoniated aerosols worsen urban air quality, influence the global radiation budget, and affect human health. Globally, the main emission source of NH_3 is farming and agriculture (93% of EU-28 emissions; EEA, 2020), and, indeed, the European Environment Agency (EEA, 2019) indicates that NH_3 emissions from farming and agriculture are responsible for episodes of high PM concentrations across certain regions of Europe, causing exceedances of PM limit values. Lelieveld et al. (2015) estimated a large impact of this source on $PM_{2.5}$, being the leading source class in Europe, Russia, Turkey, Korea, Japan and the Eastern USA. They even concluded that this contribution makes agriculture the outdoor source behind the largest impact on mortality in these regions.

It can be then inferred that when NH_3 abundance is the driving factor in secondary $PM_{2.5}$ formation, a reduction of NH_3 emissions can lead to an important air quality improvement. This could be especially true in urban environments, with typically higher NOx and SO_2 concentrations. In this line, Backes et al. (2016) found that a reduction of NH_3 emissions by 50% lead to a 24% decrease of the total $PM_{2.5}$ concentrations in northwest Europe, using the SMOKE for Europe and CMAQ model systems. The observed reduction was mainly determined by reduced formation of NH_4NO_3. In a study carried out in Munich, authors highlighted that high NH_3 emissions from surrounding agricultural areas, together with large amounts of NOx from road traffic, play a key role for secondary particle formation within the city (Ehrnsperger et al., 2021). Considering that the secondary inorganic aerosol fraction can contribute to the total observed particle mass at similar or even higher levels than the primary fraction (Amato et al., 2016; Veld MI' et al., 2021), assessing secondary particles precursors seem critical to develop effective action plans against $PM_{2.5}$.

Several potential non-agricultural NH_3 sources are present in urban environments, including road traffic, industrial production, human and pets' excretions, sewage, landfill, coal combustion and biomass burning (Sutton et al., 2000). In fact, a number of studies have concluded on high NH_3 concentrations in densely populated areas (e.g. Perrino and Catrambone, 2004; Anatolaki and Tsitouridou, 2007; Alebic-Juretic, 2008; Behera and Sharma, 2010; Reche et al., 2012, 2015; Pandolfi et al., 2012). These sources form a minor part of the emissions globally, but they might be very relevant locally. The assessment of the contribution of these sources is complicated and required further efforts.

Regarding trends on traffic emissions, the introduction of three-way catalytic converters in gasoline vehicles, together with the adoption of selective catalytic reduction (SCR) by the use of urea or NH_3 to diesel exhaust controls, are thought to be the source of NH_3 in vehicular plumes (Huai et al., 2003; Heeb et al., 2011; Suarez-Bertoa et al., 2014). Isotopic evidence for elevated fossil fuel sources of aerosol ammonium in the urban atmosphere has been identified in recent studies (Pan et al., 2018, 2020; Gu et al., 2022). Elser et al. (2018) described that traffic emissions clearly dominated the city enhancements of NH_3 in three European cities (up to 61% of ammonia in cities is related to traffic), while Amanatidis et al. (2014) concluded that the introduction of SCR also leads to particle formation in the exhaust, affecting total exhaust particle number and size distribution. These consequences highlight that it is essential to jointly evaluate plans for abating different air pollutants, in order to avoid unwanted effects.

It can be stated that there are many pending challenges in NH_3 understanding and control. According to the European commission, NH_3 emissions have decreased less than other National Emission Ceilings Directive (NECD) pollutants. Between 1990 and 2017, NH_3 emissions decreased by approximately 23% in the EU-28 and 18% in the EEA-33. However, emissions have increased each year since 2014 (EEA, 2019). Recent studies have even concluded on a worldwide increase of 12.8 ± 1.3% over the last 11 years (Van Damme et al., 2021), determined by large increases in east Asia (5.80 ± 0.61% increase per year), western and central Africa (2.58 ± 0.23 $\%yr^{-1}$), North America (2.40 ± 0.45 $\%yr^{-1}$) and western and southern Europe (1.90 ± 0.43 $\%yr^{-1}$). In addition, the impact of urban emissions is not being adequately addressed so far, with very few European countries having established a systematic measurement network, partly due to a lack of a standard quantification method. All of this creates uncertainty in NH_3 emission inventories, which could lead to inaccuracies in predicting future $PM_{2.5}$ concentration trends.

Accordingly, the objective of this work is to quantify and compare the changes in NH_3 concentrations from 2011 to 2020 in different backgrounds located in the northeast of Spain, considered a major European NH_3 hotspot (Van Damme et al., 2018). The possible consequences in the evolution of secondary inorganic fine aerosols is discussed. An evaluation of the state of NH_3 measurements in Europe, based on data reported by the European Environmental Agency (EEA, 2021), is also presented.

2. Methodology

2.1. Monitoring sites

Four air quality and climate research monitoring sites in NE Spain were selected to collect data, representing the traffic (Traffic) and the urban background of Barcelona (Urban, 70 m a.s.l.), the regional/rural background (Regional), approximately 40 km to the NE of the city (El Brull, Montseny, MSY, 720 m a.s.l., ACTRIS-GAW), and the mountain background (Mountain), at the high-altitude Montsec station, located approximately 175 km from Barcelona in the Pre-Pyrenean Range (MSA, 1592 m a.s.l., ACTRIS-GAW). The meteorology and main air pollution sources of this region are described in detail elsewhere (Millán et al., 1997; Pérez et al., 2010; Ripoll et al., 2014, 2015; Minguillón et al., 2015; Amato et al., 2016; Querol et al., 2016; Veld MI' et al., 2021).

In brief, the meteorology of this region during the winter is influenced by the presence of the Azores high pressure system, which promotes westerly trade winds, causing existing air masses to be replaced with clean Atlantic air masses. During the warm seasons, the typical Mediterranean climate prevails, with dry conditions. The weak pressure gradients in summer ensue local circulations with the subsequent accumulation of pollutants (Millán et al., 1997).

The mountain site is under free tropospheric influence, although it may receive regional pollutants during the summer time and/or under the influence of mountain breezes. The rural station is in a densely forested area, relatively far from urban and industrial areas, but it can be impacted by anthropogenic emissions under anticyclonic atmospheric

conditions. Transboundary intrusions of natural and anthropogenic aerosols from Europe and N Africa can affect both stations.

The traffic and urban background sites are located in Barcelona, a densely populated city, affected by emissions from traffic, industry and with one of the major harbors in the Mediterranean. Dispersion of pollutants in the city is governed by sea breezes.

2.2. NH_3 measurement method

A high sensitivity badge-type passive sampler (ALPHA; Tang et al., 2001) was employed for measurements of atmospheric NH_3. Details of the ALPHA samplers have been widely described elsewhere (Sutton et al., 2004; Schmidt et al., 2010; Vogt et al., 2013; Reche et al., 2012, 2015). Main characteristics of the sampling devices are reported in Table 1. Atmospheric NH_3 concentrations were calculated using an uptake rate provided by the manufacturer (3.24×10^{-3} m^3 h^{-1}). Information on samples treatment and analysis, as well as on quality control procedures are reported in Reche et al. (2015). 105 blank samples were analyzed during the sampling period, with concentrations ranging between 0.02 and 0.25 ppm.

Ammonia measurements span between years 2011 and 2020 (including COVID-19 scenario), except at the traffic site, where measurements were performed from 2014 to 2018. Samplers were located at a sampling height of approx. 3.5 m above ground and exposed during 2–4 weeks each.

2.3. Ancillary measurements

Real time gaseous pollutants measurements, NO, NO_2 (SIR S-5012), CO (Ecotech EC 9830), O_3 (SIR S-5014) and SO_2 (Thermo Scientific Model 43C), were available at a 30-min resolution, operated by Department of Environment of the Autonomous Government of Catalonia. Meteorological parameters were provided by the Department of Meteorology of University of Barcelona with a 10-min resolution.

24-h $PM_{2.5}$ samples were collected on quartz microfiber filters every four days throughout the whole sampling period, using high volume samplers (MCV, 30 m^3h^{-1}). A fraction of filter of about 75 cm^2 was water leached with de-ionized water (30 g of Milli-Q grade water) to extract the soluble fraction. The resulting solution was analyzed by ion chromatography for determination of SO_4^{2-} and NO_3^-, and by specific electrode for NH_4^+. An area of each sample of 1.5 cm^2 was punched to measure the levels of organic carbon (OC) and elemental carbon (EC) by thermal-optical carbon analyzer (SUNSET), using the EUSAAR 2 protocol (Cavalli et al., 2010). Concentrations were used to calculate the concentrations of organic matter (OM)+EC.

For further information, NH_3 air concentrations for all available European monitoring sites (annual statistics: mean, median, maximum and minimum), as reported by EEA (2021), were downloaded and analyzed, as well as data from Spanish air quality monitoring (AQM) stations, operated by local and regional monitoring networks and compiled by the Spanish Ministry of Environment (daily concentrations). Measurement methods are summarized in Table 2.

Table 1
Main information of the passive sampling devices used within this study.

Type	Capture solution	Usual exposure time	Uptake rate (m^3h^{-1})	Applicable studies
CEH ALPHA passive sampler-Badge type	Phosphorous acid	14–30 days	3.24×10^{-3}	Tang et al. (2001); Cape et al. (2004); Puchalski et al. (2011); Reche et al. (2015)

Table 2
Main information of the NH_3 measurement methods employed in different countries, as reported by EEA.

Country	Station type	Number of stations	Included years	NH_3 Measurement Method
Bulgaria	Urban	1	2013–2019	Chemiluminescence
	Suburban	1	2013–2019	Chemiluminescence
Germany	Rural	7	2013–2019	Active absorbent-Ion chromatography
	Rural	4	2013–2019	Chemiluminescence
	Traffic	1	2016–2017	Chemiluminescence
Italy	Suburban-Industrial	1	2014	Chemiluminescence
Netherlands	Rural	9	2013–2015	Potentiometry
Spain	Suburban-Industrial	1	2019	na
	[a]Traffic	2	2013–2020	Chemiluminescence
Sweden	Rural	4	2012–2019	Active absorbent-Spectrophotometry

[a] Data compiled by the Spanish Ministry of Environment.

2.4. Statistical methods

The acquired data were prepared and exported to the R environment. The Rpart package for classification and regression trees (CART) and the air pollution analysis package for R, openair (Carslaw and Ropkins, 2012), were used. Openair includes the function for the Mann–Kendall (MK) test with the Theil-Sen estimator.

CART are used in data mining in order to develop a model that predicts the value of a dependent variable based on the values of multiple inputs. The Rpart method (Brieman et al. 1984) was used in this study to plot classification trees. It has been previously applied in studies in different areas (Zhao et al., 2018; Cheng et al., 2018; Barlin et al., 2013) and proved to be an efficient technique to fit a connection between numerical variables, partitioning the target variable by a range of values of the explanatory variables.

The object of the Mann–Kendall (MK) test (Mann, 1945; Kendall, 1975; Gilbert, 1987) is to statistically assess whether there is a monotonic upward or downward trend of the variable of interest with time. A monotonic upward (downward) trend means that the variable consistently increases (decreases) through time. The Mann–Kendall test tests the null hypothesis, H0, of no trend, i.e., the observations are arbitrarily ordered in time, against the alternative hypothesis, H1, where there is an increasing or decreasing monotonic trend. Data do not need to conform any particular distribution and missing data are allowed. To estimate the slope of the trend, Sen's method was used (Salmi et al., 2002).

3. Results

3.1. Status of NH_3 data availability and concentrations in Europe

Fig. 1 summarizes NH_3 concentrations reported for different countries in Europe by type of background and by year, as specified in Table 2. Data recorded in this study has also been included for comparison.

As observed, the availability of data on NH_3 concentrations is very scarce, with very few countries reporting data consistently for extensive periods. It is especially remarkable the lack of long time series at urban background sites. Due to the absence of a well-defined standard measurement method, methods differ between sites (Table 2), thus preventing comparisons between sites in open access databases.

When analyzing the data spatially, Germany and Netherlands are the countries accounting for the highest number of monitoring sites officially reporting NH_3 concentrations, with major efforts at rural environments.

Median concentrations for all countries and type of background

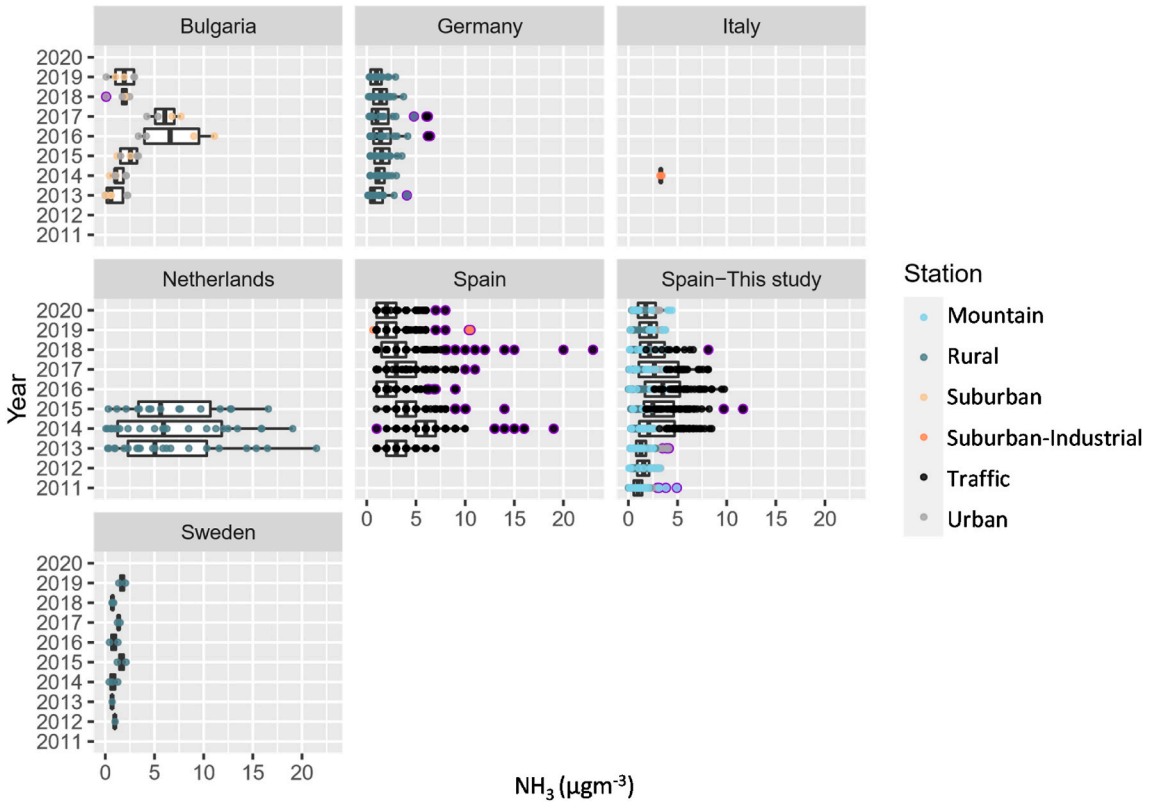

Fig. 1. Boxplots of NH_3 concentrations (μg m^{-3}) summarized by type of background and year of measurement for all countries with data availability, according to information in Table 2. Data recorded within this study is also included. Points with purple circles represent data points considered outliers. (For interpretation of the references to colour in this figure legend, the reader is referred to the Web version of this article.)

range between 0.8 and 10.3 μg m^{-3}. By type of station, the highest median concentrations are recorded at suburban-industrial sites (3.4 μg m^{-3}), followed by traffic sites (3.0 μg m^{-3}) and by urban background sites (1.9 μg m^{-3}).

A common temporal trend is not observed for the different considered sites.

3.2. Seasonality components and time trends in NE Spain

NH_3 concentrations recorded in this study are shown in Fig. 2 according to the type of background, and by month and year. The highest concentrations were recorded at the traffic site, ranging between 1.8 and 11.7 μg m^{-3} (5.3 μg m^{-3} on average). These concentrations are followed by those measured at the urban background site, with an average of 2.1 μgm^{-3} (0.1–5.0 μg m^{-3}). Mean concentrations at the mountain site are 1.6 μg m^{-3} (0.06–4.9 μg m^{-3}), while the lowest concentrations were recorded at the regional site (0.9 μg m^{-3} on average; 0.02–4.0 μg m^{-3}). The higher concentrations at the mountain site with respect to the regional one may be due to the fact that the region where the mountain station is located is one of those with a greater surface dedicated to agricultural and livestock exploitation in NE Spain (Idescat, 2022); although it is a remote site, it frequently receives regional pollutants during the summer time and/or under the influence of mountain breezes. These comparisons highlight traffic emissions as an important source of NH_3. The quantification of the traffic contribution is nonetheless uncertain due to the complex urban mix of factors interfering in the evolution, together with the rapid reactivity of this gas and dependency of the abundance of other species. Further research on nitrogen isotopic composition would be needed to delve into this question, as this method has been shown to be useful in quantifying the contribution of nonagricultural sources, especially vehicles and coal combustion (Pan et al., 2018, 2020; Gu et al., 2022). Concentrations at the traffic and urban background sites are in the range of those compiled by EEA, while concentrations reported at the regional site are generally lower (Fig. 1).

A clear seasonal pattern is observed at the mountain background, where concentrations reach their maximum during summer (Fig. 2), under higher temperatures and solar radiation, which increases convection, enhancing the growth of the PBL and the transport of anthropogenic pollutants towards high altitude sites. This pattern is probably indicating a main impact of diffuse organic sources, such as agriculture and livestock production. Concentrations increase by 80% on average during summer periods compared with winter, when they are similar to those recorded at the regional site, and markedly lower than those at the urban background (Fig. 2). Conversely, NH_3 concentrations at the traffic and urban background sites tend to be higher during winter, probably due to lower mixing layer heights, together with higher traffic emissions (Banks et al., 2014; Rivas et al., 2020). At the regional site, on the other hand, values do not vary markedly between seasons.

The assessment of the temporal trends reveals statistically significant monotonic trends at the urban background and at the mountain sites during the study period (Fig. 3), while remaining relatively constant at the regional site. At the urban background site, an all-year significant increase can be observed, with a Sen's slope of 9.4% (5.2%–14.4%) per year. Nevertheless, the season-separated analysis shows increases being especially important in summer (18.3% per year) and winter (11.9% per year). This trend could be related to a combination of regional farming/agricultural and in-city NH_3 emissions. Local NH_3 sources may include traffic, industry, sewage and garbage collection systems (Reche et al., 2012, 2015; Pandolfi et al., 2012). At the mountain site, a significant increase in concentrations over the years is evidenced during summer periods (16.0% per year), probably associated with an increase in emissions from agricultural/livestock production, mainly generated under warm conditions, giving rise to high volatilization losses. It should be noted that according to the local statistical institute (Idescat, 2022),

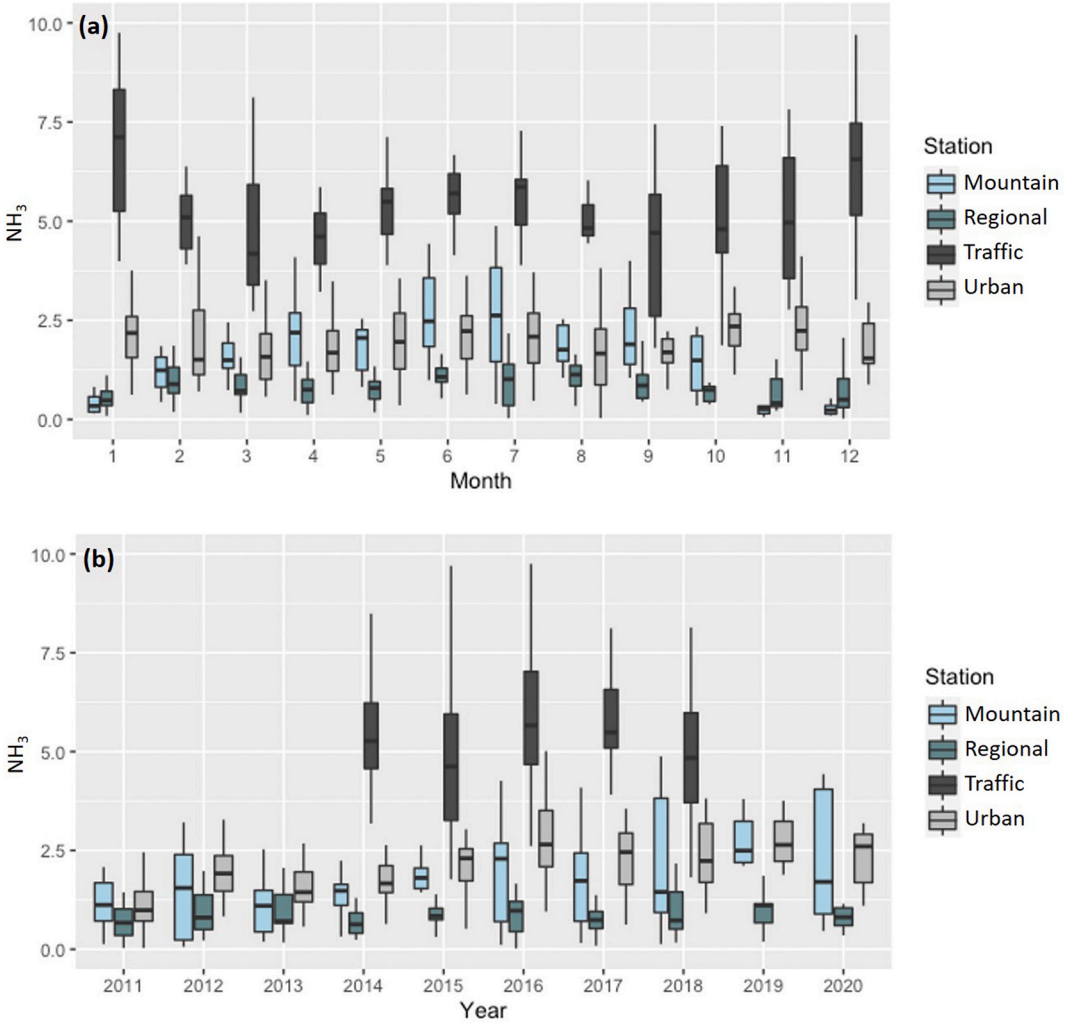

Fig. 2. Boxplots of NH_3 (μg m^{-3}) concentrations recorded in this study and summarized by type of monitoring station and (a) month, and (b) year. The line within the box plots shows the median concentrations, while the box bottom and top represent the 25th and 75th percentiles, respectively. The whiskers represent the lower (2.5th percentile) and the upper (97.5th percentile) bounds. Outliers have been removed.

there has been an increase in agricultural production in the study areas during the corresponding period.

In order to try to elucidate possible causes and implications of the detected NH_3 increases, the time series of $PM_{2.5}$ secondary compounds at both stations were simultaneously evaluated. A lack of a clear decreasing trend of NO_3^- concentrations, not coinciding with NO_2 changes (decreasing by 1.7% and 3.6% per year at the mountain and at the urban background site, respectively; Table 3), is observed. This difference in patterns could be related to the behavior of NH_3 concentrations, preventing a marked decrease of NO_3^-, which, in turn, would affect $PM_{2.5}$ concentrations. Meanwhile, SO_4^{2-} concentrations do seem to respond more directly to changes in SO_2 at both sites, decreasing by 4.03–5.27% per year (Table 3), leading to more NH_3 available to react with HNO_3.

Less formation of acidic SO_4 and NO_3, due to reduced SO_2 and NO_x emissions, provide less substrate to interact with NH_3 and form particulate ammonium species. Thus, concentrations of NH_3 can have partly increased due to this decrease in consumption, especially by H_2SO_4. Nonetheless, the MK algorithm was also applied to the sum of NH_3+NH_4^+ concentrations, obtaining results that are in line with those obtained for NH_3 (Table 3), suggesting that a reduced consumption could not explain the whole NH_3 increase observed in this study and that an increase in emissions is likely to have occurred. In addition, the season-separated trend analysis indicates that NH_3 concentrations did not directly respond to changes in NH_4^+ concentrations, with NH_3 increasing the most in winter and summer, when NH_4^+ decreased the least (Fig. 3 and Table 3).

It could be therefore deduced that the assessment of NH_3 concentrations could be useful in developing strategies to reduce $PM_{2.5}$ trends, especially in urban environments, if considering the general high contribution of secondary inorganic particles (Amato et al., 2016; Veld MI' et al., 2021). However, the prediction of NH_3 concentrations is subjected to a high uncertainty and complexity, as indicated by the application of a decision tree (Rpart) algorithm to find the parameters that best predict NH_3 at the urban background under study. NO, NO_2, CO, O_3, SO_2 and OM + EC concentrations, together with wind speed, wind direction, temperature and relative humidity, were used for the analysis. Figures S1 and S3 shows that no combination of parameters could clearly predict significant differences in NH_3 concentrations, as values at the different nodes are not representative of the complete data distribution, which could be partly due to the low temporal resolution availability in this work, along with the complexity of the intrinsic properties of this pollutant. O_3, OM + EC and temperature are the parameters showing a slightly better prediction performance at the urban background. In brief, the first split of the tree was determined by O_3 concentrations and therefore defined as the O_3 subject, with 88% of the dataset clustered with O_3 concentrations$\geq$34 μg m^{-3}. Higher O_3 subjects were segregated based on OM + EC, while lower O_3 were segregated

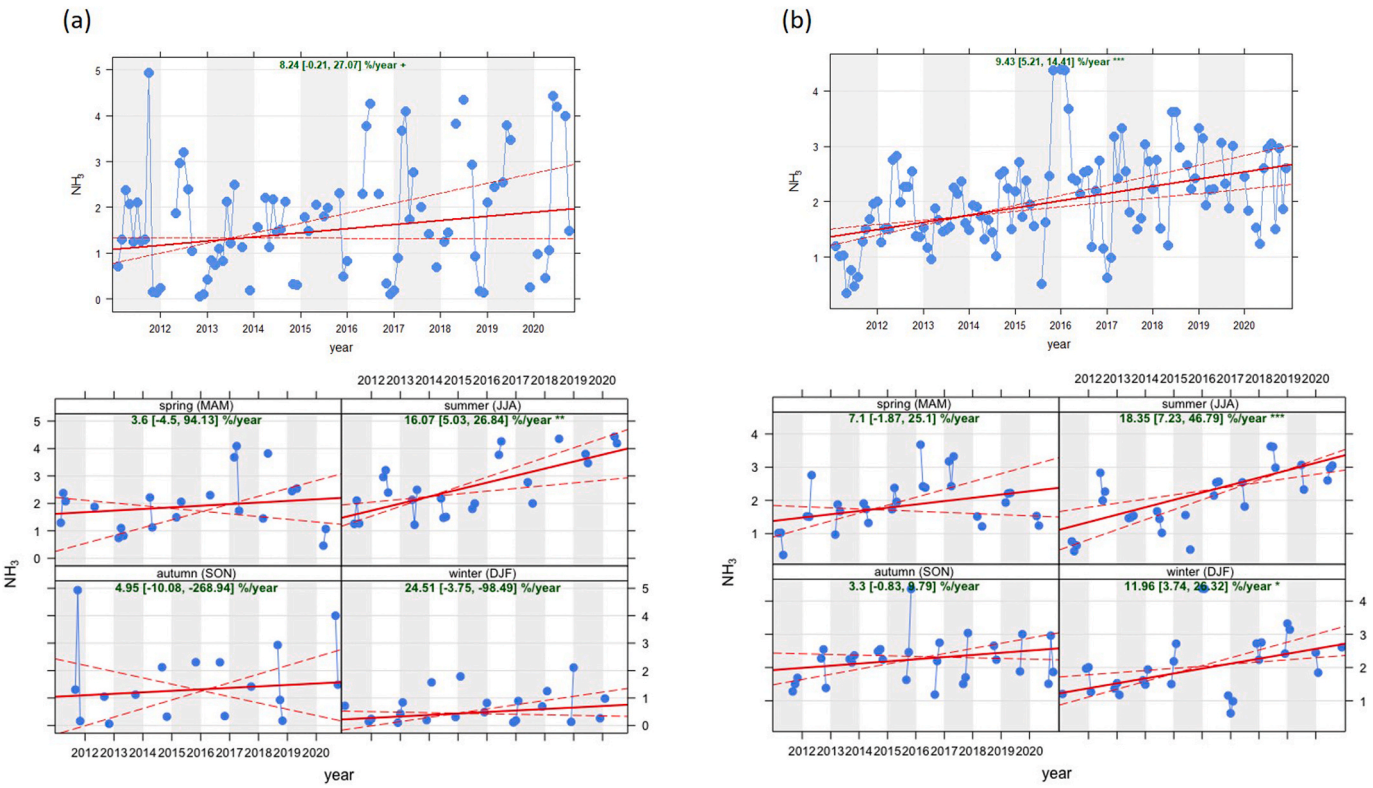

Fig. 3. Mann-Kendall Trend Test applied to NH_3 concentrations (μg m^{-3}) at the mountain (a) and urban background (b) sites for the complete period (top) and by season (bottom). Sen's slope of 2011–2020 data are indicated in green, expressed as an average annual percent change. $p < 0.001 = ***$, $p < 0.01 = **$, $p < 0.05 = *$and $p < 0.1 = +$. (For interpretation of the references to colour in this figure legend, the reader is referred to the Web version of this article.)

Table 3
Sen's slope of 2011–2020 data at the mountain and at the urban background sites, expressed as an average annual percent change. All year (January–December) and season-separated data are presented. Slopes for variables with non-significant monotonic trends are not shown (indicated with a hyphen). $p < 0.001 = ***$, $p < 0.01 = **$, $p < 0.05 = *$ and $p < 0.1 = +$. DJF (December, January, February), MAM (March, April, May), JJA (June, July, August), SON (September, October, November).

Site	Variable	All year (% $year^{-1}$)	DJF (% $year^{-1}$)	MAM (% $year^{-1}$)	JJA (% $year^{-1}$)	SON (% $year^{-1}$)
MOUNTAIN	$NH_3+NH_4^+$	–	–	–	10.01 (1.15–20.36)*	–
	NH_4^+	−6.17 (−8.2,-3.59)***	–	−8.03 (−10.02,-3.64)***	−4.63 (−7.82,-0.73)*	−6.55 (−9.99,-1.03)*
	SO_4^{2-}	−4.03 (−6.8,-0.55)*	−4.6 (−7.34,0.36)+	–	−2.48 (−4.7,-0.33)*	−6.86 (−9.29,-2.67)*
	NO_3^-	–	–	–	–	–
	SO_2	−2.04 (−3.17,-0.7)**	–	−2.97 (−6.56,-0.31)*	−2.84 (−4.93,-0.25)*	–
	NO_2	−1.74 (−2.6,-0.55)*	–	−2.34 (−4.15,-0.12)*	–	−2.42 (−3.68,-0.04)+
URBAN	$NH_3+NH_4^+$	3.81 (1.13,6.05)***	4.71 (0.66,12.77)*	–	9.89 (3.08,19.47)***	–
	NH_4^+	−4.5 (−6.01,-2.77)***	–	−6.79 (−9.68,-3.35)***	−3.21 (−5.56,0.83)+	−5.14 (−8.31,-1.61)*
	SO_4^{2-}	−5.27 (−6.56,-3.2)***	−2.83 (−6,0.89)+	−6.06 (−8.17,-3.71)***	−4.39 (−5.67,-2.29)***	−6.72 (−9.26,-3.94)***
	NO_3^-	–	–	–	–	–
	SO_2	−4.01 (−5.21,-2.43)***	−2.71 (−4.82,0.42)+	–	−4.45 (−5.98,-0.63)*	−6.71 (−8.94,-2.41)***
	NO_2	−3.66 (−4.75,-2.53)***	−3.27 (−4.8,-0.71)**	−4.17 (−6.91,-1.63)**	–	−4.16 (−5.36,-2.51)**

according to temperature. Wind speed, SO_2 and NO_X were seen as secondary predictor variables. The R-squared coefficient of the linear regression between real and predicted measurements is 0.41 (p-value<0.001; Figure S1) when considering all nodes of the decision tree. If the tree is pruned according to the complexity parameter having the least cross-validated error (Figure S2), the R-squared coefficient is significantly lower ($R^2 = 0.24$, p-value<0.001; Figure S3). It is worth mentioning that the decision tree algorithm is here intended to be used as a step to generate hypothesis about joint effects that could exist in the data in order to decide future analysis/measurement strategies. In this study, results indicate the need for highly temporally and spatially resolved NH_3 concentrations for an accurate understanding of their sources and patterns.

Another indication of the complexity of factors influencing NH_3 at the urban background is deduced by the study of the effect of the Covid-19 scenario. NH_3 concentrations show an average reduction during March–December 2020 compared with March–December 2019 of 15%, which is lower than that observed for primary pollutants in the same environment, especially traffic-related ones (Querol et al., 2021). NH_3 concentrations were, in fact, very similar during summer 2020 compared with 2019, while traffic tracers, such as NO_2, show differences of around 40% (Figure S4). The different behavior of NH_3 could be due to the combination of: (a) less consumption by H_2SO_4 during summer, when the highest differences in NH_4^+ and SO_4^{2-} between 2019 and 2020 were recorded (around 40% lower in 2020, Figure S5), (b) influence of regional agricultural/livestock emissions, and (c) lack of decrease of local non-traffic sources, such as sewage and landfill emissions. Conversely, it is also remarkable the significant decrease of NH_3 concentrations during spring (35% on average) and winter 2020 (30% on average) (Figure S4), periods with the greatest activity restrictions,

suggesting an important role of local sources on NH_3 concentrations. These differences between years were especially noteworthy when considering that they occurred while very similar NH_4^+ concentrations were maintained (Figure S5), indicating that NH_3 concentrations in 2020 were sufficient to preserve similar concentrations of secondary inorganic particles, even under a scenario of very reduced NO_2 and SO_2 concentrations.

4. Conclusions

Ammonia-induced particle formation is an environmental problem that is not fully addressed by current regulations. Shortcomings include the lack of reduction strategies for NH_3 in urban air pollution mitigation plans and of exhaust NH_3 limits for light duty vehicles. These omissions can contribute to errors in assessing $PM_{2.5}$ trends and effectiveness of action plans, considering that nitrate and sulfate aerosols are a key component of $PM_{2.5}$.

A review of open data of NH_3 concentrations, as published by the European Environment Agency (EEA, 2021), highlights that few countries have established systematic networks, especially at urban environments, where long time series are rarely available. In addition, a common standard measurement method is not established. All this contributes to uncertainties in NH_3 emission inventories.

With this context, the aim of this work was to evaluate a ten-years dataset on multi-site NH_3 concentrations in NE Spain, using diffusion tubes, in order to describe patterns and discuss possible implications. Mean NH_3 concentrations range between 0.9 and 5.3 μg m^{-3}, with the highest concentrations recorded at the traffic site, followed by the urban background site, the mountain site and, finally, the regional site. Although information is scarce, concentrations at the traffic and urban background could be considered similar to those reported in other stations in Europe, while concentrations at the regional site are systematically lower. A statistically significant temporal trend was detected at the urban background site after applying the MK algorithm, where NH_3 concentrations increased by 9.4% per year. Causes of this increase could include both regional and in-city sources, together with an expected lower consumption by HNO_3 and, especially, H_2SO_4 due to the reduction of SO_2 and NO_2 concentrations over the years. A season-based MK analysis also showed an increase in NH_3 concentrations at the mountain site during summer months (16.0% per year), maybe mainly linked to agricultural/livestock emissions. These NH_3 increases could have been partly responsible for a lack of parallelism between the decrease of NO_2 concentrations and the evolution of NO_3^- concentrations, which have remained relatively constant during the last years. This would mean that controlling NH_3 emissions would be necessary to achieve the objectives of action plans for $PM_{2.5}$. The major challenge is then dealing with the complexity of factors influencing NH_3 behavior at urban backgrounds, which would need high quality temporally and spatially resolved measurements.

Author statement

Cristina Reche: sampling; formal analysis; data treatment; writing of the original manuscript draft and revision of the manuscript. **Noemí Pérez**: conceptualization; sampling and revision of the manuscript. **Andrés Alastuey**: conceptualization; revision of the manuscript; resources and funding acquisition. **Nuria Cots**: conceptualization; sampling and revision of the manuscript. **Eva Pérez**: conceptualization; sampling and revision of the manuscript. **Xavier Querol**: conceptualization; supervision; revision of the manuscript; resources and funding acquisition. All authors have read and approved the final article.

Declaration of competing interest

The authors declare that they have no known competing financial interests or personal relationships that could have appeared to influence the work reported in this paper.

Data availability

Data will be made available on request.

Acknowledgements

The present work was supported by European Union's Horizon 2020 research and innovation programme under grant agreement 101036245 (RI-URBANS); the "Agencia Estatal de Investigación" from the Spanish Ministry of Science and Innovation, and FEDER funds, under the projects CAIAC (PID2019-108990RB-I00) and HOUSE (CGL2016-78594-R); and the Generalitat de Catalunya (AGAUR 2017 SGR41) and the Direcció General de Territori.

Appendix A. Supplementary data

Supplementary data to this article can be found online at https://doi.org/10.1016/j.chemosphere.2022.135347.

References

Alebic-Juretic, A., 2008. Airborne ammonia and ammonium within the Northern Adriatic area, Croatia. Environ. Pollut. 154, 439–447.

Amanatidis, S., Ntziachristos, L., Giechaskiel, B., Bergmann, A., Samaras, Z., 2014. Impact of selective catalytic reduction on exhaust particle formation over excess ammonia events. Environ. Sci. Technol. 48 https://doi.org/10.1021/es502895v.

Amato, F., Alastuey, A., Karanasiou, A., Lucarelli, F., Nava, S., Calzolai, G., Severi, M., Becagli, S., Gianelle, V.L., Colombi, C., Alves, C., Custódio, D., Nunes, T., Cerqueira, M., Pio, C., Eleftheriadis, K., Diapouli, E., Reche, C., Minguillón, M.C., Manousakas, M.I., Maggos, T., Vratolis, S., Harrison X, R.M., Querol, X., 2016. AIRUSE-LIFE+: a harmonized PM speciation and source apportionment in five southern European cities. Atmos. Chem. Phys. 16, 3289–3309. https://doi.org/10.5194/acp-16-3289-2016.

Anatolaki, Ch, Tsitouridou, R., 2007. Atmospheric deposition of nitrogen, sulfur and chloride in Thessaloniki, Greece. Atmos. Res. 85, 413e428.

Backes, A.M., Aulinger, A., Bieser, J., Matthias, V., Quante, M., 2016. Ammonia emissions in Europe, part II: how ammonia emision abatement strategies affect secondary aerosols. Atmos. Environ. 126, 153–161.

Banks, R., Tiana-Alsina, J., Baldasano, J., Rocadenbosch, F., 2014. Retrieval of boundary layer height from lidar using extended Kalman filter approach, classic methods, and backtrajectory cluster analysis. Proc. SPIE 9242. https://doi.org/10.1117/12.2072049.

Barlin, J.N., Zhou, Q., Clair, C.M.S., Iasonos, A., Soslow, R.A., Alektiar, K.M., Hensley, M. L., Leitao Jr., M.M., Barakat, R.R., Abu-Rustum, N.R., 2013. Classification and regression tree (CART) analysis of endometrial carcinoma: seeing the forest for the trees. Gynecol. Oncol. 130 (3), 452–456. https://doi.org/10.1016/j.ygyno.2013.06.009.

Behera, S.N., Sharma, M., 2010. Investigating the potential role of ammonia in ion chemistry of fine particulate matter formation for an urban environment. Sci. Total Environ. 408, 3569–3575.

Breiman, L., Friedman, J., Olshen, R., Stone, C., 1984. Classification and Regression Trees. Wadsworth, Monterey, CA.

Cape, J.N., Tang, Y.S., van Dijka, N., Love, L., Sutton, M.A., Pame, S.C.F., 2004. Concentrations of ammonia and nitrogen dioxide at roadside verges, and their contribution to nitrogen deposition. Environ. Pollut. 132, 469–478.

Carslaw, D.C., Ropkins, K., 2012. Openair — an R package for air quality data analysis. Environ. Model. Software 27–28, 52–61. https://doi.org/10.1016/j.envsoft.2011.09.008. ISSN 1364-8152.

Cavalli, F., Viana, M., Yttri, K.E., Genberg, J., Putaud, J.-P., 2010. Toward a standardized thermal-optical protocol for measuring atmospheric organic and elemental carbon: the EUSAAR Protocol Atmos. Meas. Tech. 3, 79–89.

Cheng, Z., Nakatsugawa, M., Chen, H., Robertson, S.P., Hui, X., Moore, J.A., Bowers, M. R., Kiess, A.P., Page, B.R., Burns, L., 2018. Evaluation of classification and regression tree (CART) model in weight loss prediction following head and neck cancer radiation therapy. Adv. Radiat. Oncol. 3 (3), 346–355. https://doi.org/10.1016/j.adro.2017.11.006.

Elser, M., El-Haddad, Imad, Maasikmets, Marek, Bozzetti, Carlo, Wolf, Robert, Ciarelli, Giancarlo, Slowik, Jay G., Richter, Rene, Teinemaa, Erik, Hüglin, Christoph, Baltensperger, Urs, André, S., Prévôt, H., 2018. High contributions of vehicular emissions to ammonia in three European cities derived from mobile measurements. Atmos. Environ. 175, 210–220. https://doi.org/10.1016/j.atmosenv.2017.11.030, 1352-2310.

Ehrnsperger, L., Klemm, O., 2021. Source apportionment of urban ammonia and its contribution to secondary particle formation in a mid-size European city. Aerosol Air Qual. Res. 21, 200404 https://doi.org/10.4209/aaqr.2020.07.0404.

European Environment Agency (EEA), 2019. In: Ammonia Emissions from Agriculture Continue to Pose Problems for Europe. https://www.eea.europa.eu/highlights/ammonia-emissions-from-agriculture-continue.

European Environment Agency (EEA), 2020. In: Air Quality in Europe - 2020 Report. EEA Report. https://www.eea.europa.eu/publications/air-quality-in-europe-2020-report.

European Environment Agency (EEA), 2021. In: Up-to-date Air Quality Data. https://www.eea.europa.eu/data-and-maps/explore-interactive-maps/up-to-date-air-quality-data.

Gilbert, R.O., 1987. Statistical Methods for Environmental Pollution Monitoring. Wiley, NY.

Gu, M., Pan, Y., Walters, W.W., Sun, Q., Song, L., Wang, Y., Xue, Y., Fang, Y., 2022. Vehicular emissions enhanced ammonia concentrations in winter mornings: insights from Diurnal nitrogen isotopic signatures. Environ. Sci. Technol. 56 (3), 1578–1585.

Heeb, Norbert V., Yan, Zimmerli, Jan, Czerwinski, Schmid, Peter, Zennegg, Markus, Haag, Regula, Seiler, Cornelia, Wichser, Adrian, Ulrich, Andrea, Peter, Honegger, Zeyer, Kerstin, Emmenegger, Lukas, Mosimann, Thomas, Kasper, Markus, Mayer, Andreas, 2011. Reactive nitrogen compounds (RNCs) in exhaust of advanced PM–NOx abatement technologies for future diesel applications. Atmos. Environ. 45 (18), 3203–3209. https://doi.org/10.1016/j.atmosenv.2011.02.013. ISSN 1352-2310.

Huai, TaoDurbin, Miller, Thomas D., WaynePisano, J., Sauer, John T., Rhee, Claudia G., Sam, H., Norbeck, Joseph, M., 2003. Investigation of NH3 emissions from new technology vehicles as a function of vehicle operating conditions. Environ. Sci. Technol. 37, 4841–4847.

Idescat, 2022. In: Instituto de Estadística de Cataluña. https://www.idescat.cat/pub/?id=aec&n=424&lang=es. (Accessed 19 April 2022).

Kendall, M.G., 1975. Rank Correlation Methods, fourth ed. Charles Griffin, London.

Lelieveld, J., Evans, J., Fnais, M., Giannadaki, D., Pozzer, A., 2015. The contribution of outdoor air pollution sources to premature mortality on a global scale. Nature 525, 367–371.

Mann, H.B., 1945. Non-parametric tests against trend. Econometrica 13, 163–171.

Millán, M.M., Salvador, R., Mantilla, E., Kallos, G., 1997. Photooxidant dynamics in the Mediterranean basin in summer: results from European research projects. J. Geophys. Res. 102, 8811–8823.

Minguillón, M.C., Brines, M., Pérez, N., Reche, C., Pandolfi, M., Fonseca, A.S., Amato, F., Alastuey, A., Lyasota, A., Codina, B., Lee, H.-K., Eun, H.-R., Ahn, K.-H., Querol, X., 2015. New particle formation at ground level and in the vertical column over the Barcelona area. Atmos. Res. 164–165, 118–130.

Pan, Y., Tian, S., Liu, D., Fang, Y., Zhu, X., Gao, M., Gao, J., Michalski, G., Wang, Y., 2018. Isotopic Evidence for Enhanced Fossil Fuel Sources of Aerosol Ammonium in the Urban Atmosphere, vol. 238. Environmental pollution, Barking, Essex, pp. 942–947. https://doi.org/10.1016/j.envpol.2018.03.038, 1987.

Pan, Y., Gu, M., Song, L., Tian, S., Wu, D., Walters, W., Yu, X., Lü, X., Ni, X., Wang, Y., Cao, J., Liu, X., Fang, Y., Wang, Yi, 2020. Systematic low bias of passive samplers in characterizing nitrogen isotopic composition of atmospheric ammonia. Atmos. Res. 243, 105018 https://doi.org/10.1016/j.atmosres.2020.105018.

Pandolfi, M., Amato, F., Reche, C., Alastuey, A., Otjes, R.P., Blom, M.J., Querol, X., 2012. Summer ammonia measurements in a densely populated Mediterranean city. Atmos. Chem. Phys. 12, 7557–7575. https://doi.org/10.5194/acp-12-7557-2012.

Perrino, C., Catrambone, M., 2004. Development of a variable-path-length diffusive sampler for ammonia and evaluation of ammonia pollution in the urban area of Rome, Italy. Atmos. Environ. 38, 6667e6672.

Pérez, N., Pey, J., Cusack, M., Reche, C., Querol, X., Alastuey, A., Viana, M., 2010. Variability of particle number, black carbon, and PM10, PM2.5, and PM1 levels and speciation: influence of road traffic emissions on urban air quality. Aerosol Sci. Technol. 44, 487–499.

Puchalski, M.A., Sather, M.E., Walker, J.T., Lehnmann, C.M.B., Gay, D.A., Mathew, J., Robarge, W.P., 2011. Passive ammonia monitoring in the United States: comparing three different sampling devices. J. Environ. Monit. 13, 3156–3167.

Querol, X., Alastuey, A., Reche, C., Orio, A., Pallares, M., Reina, F., Dieguez, J.J., Mantilla, E., Escudero, M., Alonso, L., Gangoiti, G., Millán, M., 2016. On the origin of the highest ozone episodes in Spain. Sci. Total Environ. 572, 379–389. https://doi.org/10.1016/j.scitotenv.2016.07.193.

Querol, X., Massagué, J., Alastuey, A., Moreno, T., Gangoiti, G., Mantilla, E., Duéguez, J. J., Escudero, M., Monfort, E., Pérez García-Pando, C., Petetin, H., Jorba, O., Vázquez, V., de la Rosa, J., Campos, A., Muñóz, M., Monge, S., Hervás, M., Javato, R., Cornide, M.J., 2021. Lessons from the COVID-19 air pollution decrease in Spain: now what? Jul 20 Sci. Total Environ. 779, 146380. https://doi.org/10.1016/j.scitotenv.2021.146380. . Epub 2021 Mar 16. PMID: 34030280.

Reche, C., Viana, M., Pandolfi, M., Alastuey, A., Moreno, T., Amato, F., Ripoll, A., Querol, X., 2012. Urban NH3 levels and sources in a Mediterranean environment. Atmos. Environ. 57, 153–164.

Reche, C., Viana, M., Karanasiou, A., Cusack, M., Alastuey, A., Artiñano, B., Revuelta, M. A., López-Mahía, P., Blanco-Heras, G., Rodríguez, S., Sánchez de la Campa, A.M., Fernández-Camacho, R., González-Castanedo, Y., Mantilla, E., Tang, Y.S., Querol, X., 2015. Urban NH3 levels and sources in six major Spanish cities. Chemosphere 119, 769–777. https://doi.org/10.1016/j.chemosphere.2014.07.097.

Ripoll, A., Pey, J., Minguillón, M.C., Pérez, N., Pandolfi, M., Querol, X., Alastuey, A., 2014. Three years of aerosol mass, black carbon and particle number concentrations at Montsec (southern Pyrenees, 1570 m a.s.l.). Atmos. Chem. Phys. 14, 4279–4295. https://doi.org/10.5194/acp-14-4279-2014.

Ripoll, A., Minguillón, M.C., Pey, J., Jimenez, J.L., Day, D.A., Sosedova, Y., Cononaco, F., Prevôt, A.S.H., Querol, X., Alastuey, A., 2015. Long-term real-time chemical characterization of submicron aerosols at Montsec (southern Pyrenees, 1570 m a.s.l.). Atmos. Chem. Phys. 15, 2935–2951. https://doi.org/10.5194/acp-15-2935-2015.

Rivas, I., Beddows, D.C.S., Amato, F., Green, D.C., Järvi, L., Hueglin, C., Reche, C., Timonen, H., Fuller, G.W., Niemi, J.V., Pérez, N., Aurela, M., Hopke, P.K., Alastuey, A., Kulmala, M., Harrison, R.M., Querol, X., Kelly, F.J., 2020. Source apportionment of particle number size distribution in urban background and traffic stations in four European cities. Environ. Int. 135 (2020) https://doi.org/10.1016/j.envint.2019.105345, 105345.

Salmi, T., Maata, A., Antilla, P., Ruoho-Airola, T., Amnell, T., 2002. Detecting Trends of Annual Values of Atmospheric Pollutants by the Mann Kendall Test and Sen's Slope Estimates – the Excel Template Application Makesens, Finnish Meteorological Institute, vol. 31. Publications on Air Quality, Helsinki, Finland.

Schmidt, R., Sughrue, E.l., 2010. NH3 and HCl impact on sulfur removal from E-Gas™ gasification streams using S Zorb Gen IV. Fuel Process. Technol. 91 (6), 582–590.

Suarez-Bertoa, R., Zardini, A.A., Astorga, C., 2014. Ammonia exhaust emissions from spark ignition vehicles over the New European Driving Cycle. Atmos. Environ. 97, 43–53.

Sutton, M.A., Dragosits, Y.S., Fowler, D., 2000. Ammonia emissions from nonagricultural sources in the UK. Atmos. Environ. 34, 855–869.

Sutton, M.A., Dragosits, U., Hellsten, S., Place, C.J., Dore, A.J., Tang, Y.S., van Dijk, N., Love, L., Fournier, N., Vieno, M., Weston, K.J., Smith, R.I., Coyle, M., Roy, D., Hall, J., Fowler, D., 2004. Ammonia emission and deposition in Scotland and its potential environmental impacts. Sci. World J. Sep 2 (4), 795–810. https://doi.org/10.1100/tsw.2004.130. PMID: 15349519; PMCID: PMC5956370.

Tang, Y.S., Cape, J.N., Sutton, M.A., 2001. Development and types of passive samplers for NH3 and NOx. In: Proceedings of the International Symposium on Passive Sampling of Gaseous Pollutants in Ecological Research, vol. 1. Science World, pp. 513–529.

Van Damme, M., Clarisse, L., Whitburn, S., Hadji-Lazaro, J., Hurtmans, D., Clerbaux, C., Coheur, P.F., 2018. Industrial and agricultural ammonia point sources exposed. Nature 564, 99–103. https://doi.org/10.1038/s41586-018-0747-1.

Van Damme, M., Clarisse, L., Franco, C., Sutton, M.A., Erisman, J.W., Kruit, R.W., et al., 2021. Global, regional and national trends of atmospheric ammonia derived from a decadal (2008-2018) satellite record. Environ. Res. Lett. 16, 5.

Veld, M.I.', Alastuey, A., Pandolfi, M., Amato, F., Pérez, N., Reche, C., Via, M., Minguillón, M.C., Escudero, M., Querol, X., 2021. Compositional changes of PM2.5 in NE Spain during 2009-2018: a trend analysis of the chemical composition and source apportionment, 795:148728 Sci. Total Environ. Nov 15. https://doi.org/10.1016/j.scitotenv.2021.148728. Epub 2021 Jun 28. PMID: 34328931.

Vogt, E., Dragosits, U., Braban, C.F., Theobald, M.R., Dore, A.J., van Dijk, N., Tang, Y.S., McDonald, C., Murray, S., Rees, R.M., Sutton, M.A., 2013. Heterogeneity of atmospheric ammonia at the landscape scale and consequences for environmental impact assessment. Environ. Pollut. 179, 120–131.

Zhao, X., Barber, S., Taylor, C.C., Milan, Z., 2018. Classification tree methods for panel data using wavelet-transformed time series. Comput. Stat. Data Anal. https://doi.org/10.1016/j.csda.2018.05.019.